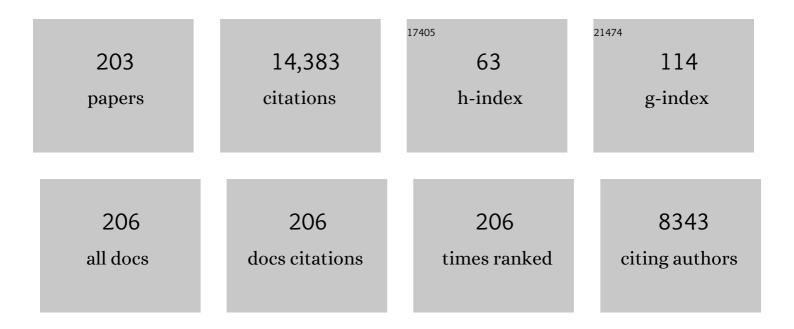
List of Publications by Year in descending order

Source: https://exaly.com/author-pdf/8437091/publications.pdf Version: 2024-02-01



#	Article	IF	CITATIONS
1	Long-Term Results of the M. D. Anderson Randomized Dose-Escalation Trial for Prostate Cancer. International Journal of Radiation Oncology Biology Physics, 2008, 70, 67-74.	0.4	1,137
2	Quantification of volumetric and geometric changes occurring during fractionated radiotherapy for head-and-neck cancer using an integrated CT/linear accelerator system. International Journal of Radiation Oncology Biology Physics, 2004, 59, 960-970.	0.4	643
3	Validation of an accelerated †demons' algorithm for deformable image registration in radiation therapy. Physics in Medicine and Biology, 2005, 50, 2887-2905.	1.6	537
4	Increased risk of biochemical and local failure in patients with distended rectum on the planning CT for prostate cancer radiotherapy. International Journal of Radiation Oncology Biology Physics, 2005, 62, 965-973.	0.4	385
5	Dosimetry tools and techniques for IMRT. Medical Physics, 2011, 38, 1313-1338.	1.6	359
6	Assessing Respiration-Induced Tumor Motion and Internal Target Volume Using Four-Dimensional Computed Tomography for Radiotherapy of Lung Cancer. International Journal of Radiation Oncology Biology Physics, 2007, 68, 531-540.	0.4	306
7	Late rectal toxicity: dose-volume effects of conformal radiotherapy for prostate cancer. International Journal of Radiation Oncology Biology Physics, 2002, 54, 1314-1321.	0.4	279
8	Design, Implementation, and inÂVivo Validation of a Novel Proton FLASH Radiation Therapy System. International Journal of Radiation Oncology Biology Physics, 2020, 106, 440-448.	0.4	274
9	Comprehensive analysis of proton range uncertainties related to patient stopping-power-ratio estimation using the stoichiometric calibration. Physics in Medicine and Biology, 2012, 57, 4095-4115.	1.6	273
10	Stereotactic Body Radiation Therapy in Centrally and Superiorly Located Stage I or Isolated Recurrent Non–Small-Cell Lung Cancer. International Journal of Radiation Oncology Biology Physics, 2008, 72, 967-971.	0.4	251
11	Quality assurance for imageâ€guided radiation therapy utilizing CTâ€based technologies: A report of the AAPM TGâ€179. Medical Physics, 2012, 39, 1946-1963.	1.6	251
12	Use of deformed intensity distributions for on-line modification of image-guided IMRT to account for interfractional anatomic changes. International Journal of Radiation Oncology Biology Physics, 2005, 61, 1258-1266.	0.4	218
13	An evidence based review of proton beam therapy: The report of ASTRO's emerging technology committee. Radiotherapy and Oncology, 2012, 103, 8-11.	0.3	212
14	Reducing metal artifacts in cone-beam CT images by preprocessing projection data. International Journal of Radiation Oncology Biology Physics, 2007, 67, 924-932.	0.4	209
15	Osteoradionecrosis and Radiation Dose to the Mandible in Patients With Oropharyngeal Cancer. International Journal of Radiation Oncology Biology Physics, 2013, 85, 415-420.	0.4	209
16	Adaptive Radiotherapy for Head-and-Neck Cancer: Initial Clinical Outcomes From a Prospective Trial. International Journal of Radiation Oncology Biology Physics, 2012, 83, 986-993.	0.4	205
17	Feasibility of sparing lung and other thoracic structures with intensity-modulated radiotherapy for non–small-cell lung cancer. International Journal of Radiation Oncology Biology Physics, 2004, 58, 1268-1279.	0.4	199
18	Intrafraction prostate motion during IMRT for prostate cancer. International Journal of Radiation Oncology Biology Physics, 2002, 53, 261-268.	0.4	193

#	Article	IF	CITATIONS
19	Report of the <scp>AAPM TG</scp> â€256 on the relative biological effectiveness of proton beams in radiation therapy. Medical Physics, 2019, 46, e53-e78.	1.6	189
20	4D Proton treatment planning strategy for mobile lung tumors. International Journal of Radiation Oncology Biology Physics, 2007, 67, 906-914.	0.4	178
21	Implementation and validation of a three-dimensional deformable registration algorithm for targeted prostate cancer radiotherapy. International Journal of Radiation Oncology Biology Physics, 2005, 61, 725-735.	0.4	168
22	Adaptive radiotherapy for head and neck cancer—Dosimetric results from a prospective clinical trial. Radiotherapy and Oncology, 2013, 106, 80-84.	0.3	168
23	Multiple regions-of-interest analysis of setup uncertainties for head-and-neck cancer radiotherapy. International Journal of Radiation Oncology Biology Physics, 2006, 64, 1559-1569.	0.4	165
24	Consensus Guidelines for Implementing Pencil-Beam Scanning Proton Therapy for Thoracic Malignancies on Behalf of the PTCOG Thoracic and Lymphoma Subcommittee. International Journal of Radiation Oncology Biology Physics, 2017, 99, 41-50.	0.4	162
25	Candidate Dosimetric Predictors of Long-Term Swallowing Dysfunction After Oropharyngeal Intensity-Modulated Radiotherapy. International Journal of Radiation Oncology Biology Physics, 2010, 78, 1356-1365.	0.4	156
26	A Beam-Specific Planning Target Volume (PTV) Design for Proton Therapy to Account for Setup and Range Uncertainties. International Journal of Radiation Oncology Biology Physics, 2012, 82, e329-e336.	0.4	145
27	Experience of ultrasound-based daily prostate localization. International Journal of Radiation Oncology Biology Physics, 2003, 56, 436-447.	0.4	144
28	Effectiveness of robust optimization in intensityâ€modulated proton therapy planning for head and neck cancers. Medical Physics, 2013, 40, 051711.	1.6	135
29	Objective assessment of deformable image registration in radiotherapy: A multiâ€institution study. Medical Physics, 2008, 35, 5944-5953.	1.6	132
30	Disease-control rates following intensity-modulated radiation therapy for small primary oropharyngeal carcinoma. International Journal of Radiation Oncology Biology Physics, 2007, 67, 438-444.	0.4	130
31	Parotid Gland Dose in Intensity-Modulated Radiotherapy for Head and Neck Cancer: Is What You Plan What You Get?. International Journal of Radiation Oncology Biology Physics, 2007, 69, 1290-1296.	0.4	130
32	Investigation of bladder dose and volume factors influencing late urinary toxicity after external beam radiotherapy for prostate cancer. International Journal of Radiation Oncology Biology Physics, 2007, 67, 1059-1065.	0.4	127
33	Physics Controversies in Proton Therapy. Seminars in Radiation Oncology, 2013, 23, 88-96.	1.0	127
34	An automatic CT-guided adaptive radiation therapy technique by online modification of multileaf collimator leaf positions for prostate cancer. International Journal of Radiation Oncology Biology Physics, 2005, 62, 154-163.	0.4	125
35	Intensity-Modulated Proton Therapy Further Reduces Normal Tissue Exposure During Definitive Therapy for Locally Advanced Distal Esophageal Tumors: A Dosimetric Study. International Journal of Radiation Oncology Biology Physics, 2011, 81, 1336-1342.	0.4	122
36	Hazards of dose escalation in prostate cancer radiotherapy. International Journal of Radiation Oncology Biology Physics, 2003, 57, 1260-1268.	0.4	121

#	Article	IF	CITATIONS
37	Image Guided Radiation Therapy (IGRT) Technologies for Radiation Therapy Localization and Delivery. International Journal of Radiation Oncology Biology Physics, 2013, 87, 33-45.	0.4	120
38	Effectiveness of noncoplanar IMRT planning using a parallelized multiresolution beam angle optimization method for paranasal sinus carcinoma. International Journal of Radiation Oncology Biology Physics, 2005, 63, 594-601.	0.4	119
39	Reduce in Variation and Improve Efficiency of Target Volume Delineation by a Computer-Assisted System Using a Deformable Image Registration Approach. International Journal of Radiation Oncology Biology Physics, 2007, 68, 1512-1521.	0.4	113
40	Comparison of 2D Radiographic Images and 3D Cone Beam Computed Tomography for Positioning Head-and-Neck Radiotherapy Patients. International Journal of Radiation Oncology Biology Physics, 2008, 71, 916-925.	0.4	112
41	Evaluation of mechanical precision and alignment uncertainties for an integrated CT/LINAC system. Medical Physics, 2003, 30, 1198-1210.	1.6	107
42	Automatic Segmentation of Whole Breast Using Atlas Approach and Deformable Image Registration. International Journal of Radiation Oncology Biology Physics, 2009, 73, 1493-1500.	0.4	102
43	Use of portal images and BAT ultrasonography to measure setup error and organ motion for prostate IMRT: implications for treatment margins. International Journal of Radiation Oncology Biology Physics, 2003, 56, 1218-1224.	0.4	101
44	Image–Guided Radiation Therapy for Non–small Cell Lung Cancer. Journal of Thoracic Oncology, 2008, 3, 177-186.	0.5	101
45	Patient-specific point dose measurement for IMRT monitor unit verification. International Journal of Radiation Oncology Biology Physics, 2003, 56, 867-877.	0.4	100
46	Patterns of Disease Recurrence Following Treatment of Oropharyngeal Cancer With Intensity Modulated Radiation Therapy. International Journal of Radiation Oncology Biology Physics, 2013, 85, 941-947.	0.4	99
47	Performance Evaluation of Automatic Anatomy Segmentation Algorithm on Repeat or Four-Dimensional Computed Tomography Images Using Deformable Image Registration Method. International Journal of Radiation Oncology Biology Physics, 2008, 72, 210-219.	0.4	98
48	Automatic registration of the prostate for computed-tomography-guided radiotherapy. Medical Physics, 2003, 30, 2750-2757.	1.6	94
49	Comparison of rectal dose–wall histogram versus dose–volume histogram for modeling the incidence of late rectal bleeding after radiotherapy. International Journal of Radiation Oncology Biology Physics, 2004, 60, 1589-1601.	0.4	94
50	Effect of anatomic motion on proton therapy dose distributions in prostate cancer treatment. International Journal of Radiation Oncology Biology Physics, 2007, 67, 620-629.	0.4	89
51	Monte Carlo simulations of the dosimetric impact of radiopaque fiducial markers for proton radiotherapy of the prostate. Physics in Medicine and Biology, 2007, 52, 2937-2952.	1.6	83
52	Proton Radiotherapy for Liver Tumors: Dosimetric Advantages Over Photon Plans. Medical Dosimetry, 2008, 33, 259-267.	0.4	83
53	FLASH Proton Radiotherapy Spares Normal Epithelial and Mesenchymal Tissues While Preserving Sarcoma Response. Cancer Research, 2021, 81, 4808-4821.	0.4	77
54	Estimation of $\hat{I} \pm / \hat{I}^2$ for Late Rectal Toxicity Based on RTOG 94-06. International Journal of Radiation Oncology Biology Physics, 2011, 81, 600-605.	0.4	76

#	Article	lF	CITATIONS
55	The Use of Rectal Balloon During the Delivery of Intensity Modulated Radiotherapy (IMRT) for Prostate Cancer. Cancer Journal (Sudbury, Mass), 2002, 8, 476-483.	1.0	75
56	Impact of respiratory motion on worst-case scenario optimized intensity modulated proton therapy for lung cancers. Practical Radiation Oncology, 2015, 5, e77-e86.	1.1	75
57	Development of methods for beam angle optimization for IMRT using an accelerated exhaustive search strategy. International Journal of Radiation Oncology Biology Physics, 2004, 60, 1325-1337.	0.4	74
58	Quantification of Prostate and Seminal Vesicle Interfraction Variation During IMRT. International Journal of Radiation Oncology Biology Physics, 2008, 71, 813-820.	0.4	74
59	Evaluation of respiratory-induced target motion for esophageal tumors at the gastroesophageal junction. Radiotherapy and Oncology, 2007, 84, 283-289.	0.3	73
60	An image correlation procedure for digitally reconstructed radiographs and electronic portal images. International Journal of Radiation Oncology Biology Physics, 1995, 33, 1053-1060.	0.4	69
61	Dose–response characteristics of low- and intermediate-risk prostate cancer treated with external beam radiotherapy. International Journal of Radiation Oncology Biology Physics, 2005, 61, 993-1002.	0.4	68
62	Dose Constraints to Prevent Radiation-Induced Brachial Plexopathy in Patients Treated for Lung Cancer. International Journal of Radiation Oncology Biology Physics, 2012, 82, e391-e398.	0.4	67
63	Roadmap: proton therapy physics and biology. Physics in Medicine and Biology, 2021, 66, 05RM01.	1.6	67
64	Dose–volume response analyses of late rectal bleeding after radiotherapy for prostate cancer. International Journal of Radiation Oncology Biology Physics, 2004, 59, 353-365.	0.4	66
65	Rapid radiographic film calibration for IMRT verification using automated MLC fields. Medical Physics, 2002, 29, 2384-2390.	1.6	64
66	Multi-Institutional Dosimetric Evaluation of Modern Day Stereotactic Radiosurgery (SRS) Treatment Options for Multiple Brain Metastases. Frontiers in Oncology, 2019, 9, 483.	1.3	64
67	Ultrasound-Based Localization. Seminars in Radiation Oncology, 2005, 15, 180-191.	1.0	62
68	Dosimetric accuracy of Kodak EDR2 film for IMRT verifications. Medical Physics, 2005, 32, 539-548.	1.6	61
69	A deformable image registration method to handle distended rectums in prostate cancer radiotherapy. Medical Physics, 2006, 33, 3304-3312.	1.6	61
70	Accuracy of two heterogeneity dose calculation algorithms for IMRT in treatment plans designed using an anthropomorphic thorax phantom. Medical Physics, 2007, 34, 1850-1857.	1.6	60
71	Late Rectal Toxicity on RTOG 94-06: Analysis Using a Mixture Lyman Model. International Journal of Radiation Oncology Biology Physics, 2010, 78, 1253-1260.	0.4	60
72	Characterization of rectal normal tissue complication probability after high-dose external beam radiotherapy for prostate cancer. International Journal of Radiation Oncology Biology Physics, 2004, 58, 1513-1519.	0.4	56

#	Article	IF	CITATIONS
73	Adaptive Radiation Therapy for Head and Neck Cancer—Can an Old Goal Evolve into a New Standard?. Journal of Oncology, 2011, 2011, 1-13.	0.6	56
74	Dosimetric benefits of robust treatment planning for intensity modulated proton therapy for base-of-skull cancers. Practical Radiation Oncology, 2014, 4, 384-391.	1.1	56
75	Beam angle optimization and reduction for intensity-modulated radiation therapy of non–small-cell lung cancers. International Journal of Radiation Oncology Biology Physics, 2006, 65, 561-572.	0.4	55
76	Speed and convergence properties of gradient algorithms for optimization of IMRT. Medical Physics, 2004, 31, 1141-1152.	1.6	53
77	Statistical Assessment of Proton Treatment Plans Under Setup and Range Uncertainties. International Journal of Radiation Oncology Biology Physics, 2013, 86, 1007-1013.	0.4	53
78	Evaluation of a contour-alignment technique for CT-guided prostate radiotherapy: an intra- and interobserver study. International Journal of Radiation Oncology Biology Physics, 2004, 59, 412-418.	0.4	50
79	Dosimetric comparison of four target alignment methods for prostate cancer radiotherapy. International Journal of Radiation Oncology Biology Physics, 2006, 66, 883-891.	0.4	49
80	Comparison of FLASH Proton Entrance and the Spread-Out Bragg Peak Dose Regions in the Sparing of Mouse Intestinal Crypts and in a Pancreatic Tumor Model. Cancers, 2021, 13, 4244.	1.7	48
81	Cluster model analysis of late rectal bleeding after IMRT of prostate cancer: A case–control study. International Journal of Radiation Oncology Biology Physics, 2006, 64, 1255-1264.	0.4	47
82	Modeling respiratory motion for reducing motion artifacts in 4D CT images. Medical Physics, 2013, 40, 041716.	1.6	47
83	Integrated beam orientation and scanningâ€spot optimization in intensityâ€modulated proton therapy for brain and unilateral head and neck tumors. Medical Physics, 2018, 45, 1338-1350.	1.6	45
84	Toward a better understanding of the gamma index: Investigation of parameters with a surfaceâ \in based	1.6	44
85	Comparison of multiâ€institutional Varian ProBeam pencil beam scanning proton beam commissioning data. Journal of Applied Clinical Medical Physics, 2017, 18, 96-107.	0.8	42
86	Changes in the Pelvic Anatomy After an IMRT Treatment Fraction of Prostate Cancer. International Journal of Radiation Oncology Biology Physics, 2007, 68, 1529-1536.	0.4	41
87	Dose sculpting with generalized equivalent uniform dose. Medical Physics, 2005, 32, 1387-1396.	1.6	40
88	Dose-response for biochemical control among high-risk prostate cancer patients after external beam radiotherapy. International Journal of Radiation Oncology Biology Physics, 2003, 56, 1234-1240.	0.4	39
89	A comparison of tumor motion characteristics between early stage and locally advanced stage lung cancers. Radiotherapy and Oncology, 2012, 104, 33-38.	0.3	39
90	Verification of radiosurgery target point alignment with an electronic portal imaging device (EPID). Medical Physics, 1997, 24, 263-267.	1.6	38

#	Article	IF	CITATIONS
91	A portal image alignment and patient setup verification procedure using moments and correlation techniques. Physics in Medicine and Biology, 1996, 41, 697-723.	1.6	37
92	Automatic contouring of brachial plexus using a multi-atlas approach for lung cancer radiation therapy. Practical Radiation Oncology, 2013, 3, e139-e147.	1.1	37
93	Lack of Correlation Between External Fiducial Positions and Internal Tumor Positions During Breath-Hold CT. International Journal of Radiation Oncology Biology Physics, 2010, 76, 1586-1591.	0.4	36
94	Position effects of acoustic micro-resonator in quartz enhanced photoacoustic spectroscopy. Sensors and Actuators B: Chemical, 2015, 206, 364-370.	4.0	36
95	Is a 3-mm intrafractional margin sufficient for daily image-guided intensity-modulated radiation therapy of prostate cancer?. Radiotherapy and Oncology, 2007, 85, 251-259.	0.3	35
96	Advantages of simulating thoracic cancer patients in an upright position. Practical Radiation Oncology, 2014, 4, e53-e58.	1.1	35
97	Experience in commissioning the halcyon linac. Medical Physics, 2019, 46, 4304-4313.	1.6	35
98	Current delivery limitations of proton PBS for FLASH. Radiotherapy and Oncology, 2021, 155, 212-218.	0.3	35
99	Retrospective analysis of 2D patient-specific IMRT verifications. Medical Physics, 2005, 32, 838-850.	1.6	34
100	Assessment of shoulder position variation and its impact on IMRT and VMAT doses for head and neck cancer. Radiation Oncology, 2012, 7, 19.	1.2	34
101	The Effect of Dental Artifacts, Contrast Media, and Experience on Interobserver Contouring Variations in Head and Neck Anatomy. American Journal of Clinical Oncology: Cancer Clinical Trials, 2007, 30, 191-198.	0.6	33
102	Effectiveness of Using Fewer Implanted Fiducial Markers for Prostate Target Alignment. International Journal of Radiation Oncology Biology Physics, 2009, 74, 1283-1289.	0.4	33
103	Anatomic Distribution of Fluorodeoxyglucose-Avid Para-aortic Lymph Nodes in Patients With Cervical Cancer. International Journal of Radiation Oncology Biology Physics, 2013, 85, 1045-1050.	0.4	33
104	Quantifying the Interfractional Displacement of the Gastroesophageal Junction During Radiation Therapy for Esophageal Cancer. International Journal of Radiation Oncology Biology Physics, 2012, 83, e273-e280.	0.4	31
105	Efficiency of respiratory-gated delivery of synchrotron-based pulsed proton irradiation. Physics in Medicine and Biology, 2008, 53, 1947-1959.	1.6	30
106	Current clinical coverage of Radiation Therapy Oncology Group-defined target volumes for postmastectomy radiation therapy. Practical Radiation Oncology, 2012, 2, 201-209.	1.1	30
107	A sixâ€year review of more than 13,000 patientâ€specific IMRT QA results from 13 different treatment sites. Journal of Applied Clinical Medical Physics, 2014, 15, 196-206.	0.8	30
108	AAPM Task Group Report 290: Respiratory motion management for particle therapy. Medical Physics, 2022, 49, .	1.6	30

#	Article	IF	CITATIONS
109	Auto-segmentation of low-risk clinical target volume for head and neck radiation therapy. Practical Radiation Oncology, 2014, 4, e31-e37.	1.1	28
110	Robust beam orientation optimization for intensityâ€nodulated proton therapy. Medical Physics, 2019, 46, 3356-3370.	1.6	28
111	Dosimetric Performance and Planning/Delivery Efficiency of a Dual-Layer Stacked and Staggered MLC on Treating Multiple Small Targets: A Planning Study Based on Single-Isocenter Multi-Target Stereotactic Radiosurgery (SRS) to Brain Metastases. Frontiers in Oncology, 2019, 9, 7.	1.3	28
112	A novel energy layer optimization framework for spotâ€scanning proton arc therapy. Medical Physics, 2020, 47, 2072-2084.	1.6	27
113	Cluster models of dose–volume effects. International Journal of Radiation Oncology Biology Physics, 2004, 59, 1491-1504.	0.4	26
114	Comparison of Treatment Volumes and Techniques in Prostate Cancer Radiation Therapy. American Journal of Clinical Oncology: Cancer Clinical Trials, 2005, 28, 618-625.	0.6	26
115	Tumor-Volume Simulation During Radiotherapy for Head-and-Neck Cancer Using a Four-Level Cell Population Model. International Journal of Radiation Oncology Biology Physics, 2009, 75, 595-602.	0.4	26
116	Do Intermediate Radiation Doses Contribute to Late Rectal Toxicity? An Analysis of Data From Radiation Therapy Oncology Group Protocol 94-06. International Journal of Radiation Oncology Biology Physics, 2012, 84, 390-395.	0.4	26
117	Daily Alignment Results of In-Room Computed Tomography–Guided Stereotactic Body Radiation Therapy for Lung Cancer. International Journal of Radiation Oncology Biology Physics, 2011, 79, 473-480.	0.4	25
118	Evaluation of Tumor Position and PTV Margins Using Image Guidance and Respiratory Gating. International Journal of Radiation Oncology Biology Physics, 2010, 76, 1578-1585.	0.4	24
119	Assessing the impact of an alternative biochemical failure definition on radiation dose response for high-risk prostate cancer treated with external beam radiotherapy. International Journal of Radiation Oncology Biology Physics, 2005, 61, 14-19.	0.4	23
120	Spine SBRT With Halcyonâ,,¢: Plan Quality, Modulation Complexity, Delivery Accuracy, and Speed. Frontiers in Oncology, 2019, 9, 319.	1.3	23
121	High-sensitivity, large dynamic range, auto-calibration methane optical sensor using a short confocal Fabry–Perot cavity. Sensors and Actuators B: Chemical, 2007, 127, 350-357.	4.0	22
122	Statistical Modeling Approach to Quantitative Analysis of Interobserver Variability in Breast Contouring. International Journal of Radiation Oncology Biology Physics, 2014, 89, 214-221.	0.4	22
123	A Super-Learner Model for Tumor Motion Prediction and Management in Radiation Therapy: Development and Feasibility Evaluation. Scientific Reports, 2019, 9, 14868.	1.6	22
124	Design and commissioning of an image-guided small animal radiation platform and quality assurance protocol for integrated proton and x-ray radiobiology research. Physics in Medicine and Biology, 2019, 64, 135013.	1.6	22
125	Cherenkov imaging for total skin electron therapy (TSET). Medical Physics, 2020, 47, 201-212.	1.6	22
126	A pencil-beam photon dose algorithm for stereotactic radiosurgery using a miniature multileaf collimator. Medical Physics, 1998, 25, 841-850.	1.6	21

#	Article	IF	CITATIONS
127	Anatomic distribution of [18 F] fluorodeoxyglucose-avid lymph nodes in patients with cervical cancer. Practical Radiation Oncology, 2013, 3, 45-53.	1.1	21
128	Automated Knowledge-Based Intensity-Modulated Proton Planning: An International Multicenter Benchmarking Study. Cancers, 2018, 10, 420.	1.7	21
129	Current State of Image Guidance in Radiation Oncology: Implications for PTV Margin Expansion and Adaptive Therapy. Seminars in Radiation Oncology, 2018, 28, 238-247.	1.0	21
130	Initial Evaluation of a Novel Cone-Beam CT-Based Semi-Automated Online Adaptive Radiotherapy System for Head and Neck Cancer Treatment – A Timing and Automation Quality Study. Cureus, 2020, 12, e9660.	0.2	21
131	Medical Physics, 2012, 39, 5136-5144.	1.6	20
132	Impact of Multi-leaf Collimator Parameters on Head and Neck Plan Quality and Delivery: A Comparison between Halcyonâ,,¢ and Truebeam® Treatment Delivery Systems. Cureus, 2018, 10, e3648.	0.2	20
133	Improving accuracy of electron density measurement in the presence of metallic implants using orthovoltage computed tomography. Medical Physics, 2008, 35, 1932-1941.	1.6	19
134	Metabolic Imaging Biomarkers of Postradiotherapy Xerostomia. International Journal of Radiation Oncology Biology Physics, 2012, 83, 1609-1616.	0.4	19
135	Perturbation of waterâ€equivalent thickness as a surrogate for respiratory motion in proton therapy. Journal of Applied Clinical Medical Physics, 2016, 17, 368-378.	0.8	19
136	Deep learning for automatic target volume segmentation in radiation therapy: a review. Quantitative Imaging in Medicine and Surgery, 2021, 11, 4847-4858.	1.1	19
137	Increase in Superficial Dose in Whole-Breast Irradiation With Halcyon Straight-Through Linac Compared With Traditional C-arm Linac With Flattening Filter: InÁvivo Dosimetry and Planning Study. Advances in Radiation Oncology, 2020, 5, 120-126.	0.6	18
138	A sensitivity-guided algorithm for automated determination of IMRT objective function parameters. Medical Physics, 2006, 33, 2935-2944.	1.6	17
139	A serial 4DCT study to quantify range variations in charged particle radiotherapy of thoracic cancers. Journal of Radiation Research, 2014, 55, 309-319.	0.8	17
140	Development of Ultra-High Dose-Rate (FLASH) Particle Therapy. IEEE Transactions on Radiation and Plasma Medical Sciences, 2022, 6, 252-262.	2.7	17
141	Management of Motion and Anatomical Variations in Charged Particle Therapy: Past, Present, and Into the Future. Frontiers in Oncology, 2022, 12, 806153.	1.3	17
142	Dose to Highly Functional Ventilation Zones Improves Prediction of Radiation Pneumonitis for Proton and Photon Lung Cancer Radiation Therapy. International Journal of Radiation Oncology Biology Physics, 2020, 107, 79-87.	0.4	16
143	Characterization of a highâ€resolution 2D transmission ion chamber for independent validation of proton pencil beam scanning of conventional and FLASH dose delivery. Medical Physics, 2021, 48, 3948-3957.	1.6	16
144	Dosimetric verification for intensity-modulated radiotherapy of thoracic cancers using experimental and Monte Carlo approaches. International Journal of Radiation Oncology Biology Physics, 2006, 66, 939-948.	0.4	15

#	Article	IF	CITATIONS
145	Linear energy transfer weighted beam orientation optimization for intensityâ€modulated proton therapy. Medical Physics, 2021, 48, 57-70.	1.6	15
146	High-dose intensity modulated radiation therapy for prostate cancer. Current Urology Reports, 2004, 5, 197-202.	1.0	14
147	A novel patch-field design using an optimized grid filter for passively scattered proton beams. Physics in Medicine and Biology, 2007, 52, N265-N275.	1.6	14
148	The precision of respiratory-gated delivery of synchrotron-based pulsed beam proton therapy. Physics in Medicine and Biology, 2010, 55, 7633-7647.	1.6	14
149	Fast range-corrected proton dose approximation method using prior dose distribution. Physics in Medicine and Biology, 2012, 57, 3555-3569.	1.6	14
150	A technique to use CT images for <i>in vivo</i> detection and quantification of the spatial distribution of radiationâ€induced esophagitis. Journal of Applied Clinical Medical Physics, 2013, 14, 91-98.	0.8	14
151	Learning anatomy changes from patient populations to create artificial CT images for voxelâ€level validation of deformable image registration. Journal of Applied Clinical Medical Physics, 2016, 17, 246-258.	0.8	14
152	Dosimetric impact and detectability of multiâ€leaf collimator positioning errors on Varian Halcyon. Journal of Applied Clinical Medical Physics, 2019, 20, 47-55.	0.8	14
153	Initial Clinical Experience Treating Patients with Breast Cancer on a 6-MV Flattening-Filter-Free O-Ring Linear Accelerator. Advances in Radiation Oncology, 2019, 4, 571-578.	0.6	14
154	Influence of intravenous contrast agent on dose calculation in proton therapy using dual energy CT. Physics in Medicine and Biology, 2019, 64, 125024.	1.6	14
155	Improving Soft-Tissue Contrast in Four-Dimensional Computed Tomography Images of Liver Cancer Patients Using a Deformable Image Registration Method. International Journal of Radiation Oncology Biology Physics, 2008, 72, 201-209.	0.4	13
156	A statistical modeling approach for evaluating auto-segmentation methods for image-guided radiotherapy. Computerized Medical Imaging and Graphics, 2012, 36, 492-500.	3.5	13
157	A novel doseâ€based positioning method for CT imageâ€guided proton therapy. Medical Physics, 2013, 40, 051714.	1.6	13
158	Robust optimization for intensityâ€modulated proton therapy with soft spot sensitivity regularization. Medical Physics, 2019, 46, 1408-1425.	1.6	13
159	Dosimetric Characterization of the Dual Layer MLC System for an O-Ring Linear Accelerator. Technology in Cancer Research and Treatment, 2019, 18, 153303381988364.	0.8	12
160	Inter-fraction robustness of intensity-modulated proton therapy in the post-operative treatment of oropharyngeal and oral cavity squamous cell carcinomas. British Journal of Radiology, 2020, 93, 20190638.	1.0	12
161	Piezo-enhanced acoustic detection module for mid-infrared trace gas sensing using a grooved quartz tuning fork. Optics Express, 2019, 27, 35267.	1.7	12
162	The delivery of IMRT with a single physical modulator for multiple fields: a feasibility study for paranasal sinus cancer. International Journal of Radiation Oncology Biology Physics, 2004, 58, 876-887.	0.4	11

#	Article	IF	CITATIONS
163	Use of fractional dose–volume histograms to model risk of acute rectal toxicity among patients treated on RTOG 94-06. Radiotherapy and Oncology, 2012, 104, 109-113.	0.3	11
164	Anisotropic Margin Expansions in 6 Anatomic Directions for Oropharyngeal Image Guided Radiation Therapy. International Journal of Radiation Oncology Biology Physics, 2013, 87, 596-601.	0.4	11
165	Characterization of the Megavoltage Cone-Beam Computed Tomography (MV-CBCT) System on HalcyonTM for IGRT: Image Quality Benchmark, Clinical Performance, and Organ Doses. Frontiers in Oncology, 2019, 9, 496.	1.3	11
166	A CT-based software tool for evaluating compensator quality in passively scattered proton therapy. Physics in Medicine and Biology, 2010, 55, 6759-6771.	1.6	10
167	Whole Breast Irradiation with Halcyonâ,,¢ 2.0: Workflow and Efficiency of Field-in-Field Treatment with Dynamic Beam Flattening Technique and kV Cone Beam Computed Tomography. Cureus, 2018, 10, e3510.	0.2	10
168	Impact of fractionation and number of fields on dose homogeneity for intra-fractionally moving lung tumors using scanned carbon ion treatment. Radiotherapy and Oncology, 2016, 118, 498-503.	0.3	9
169	Evaluation of an a priori scatter correction algorithm for cone-beam computed tomography based range and dose calculations in proton therapy. Physics and Imaging in Radiation Oncology, 2020, 16, 89-94.	1.2	9
170	Field-Specific Intensity-modulated Proton Therapy Optimization Technique for Breast Cancer Patients with Tissue Expanders Containing Metal Ports. Cureus, 2017, 9, e1698.	0.2	8
171	Digital reconstruction of high-quality daily 4D cone-beam CT images using prior knowledge of anatomy and respiratory motion. Computerized Medical Imaging and Graphics, 2015, 40, 30-38.	3.5	7
172	On-line dose-guidance to account for inter-fractional motion during proton therapy. Physics and Imaging in Radiation Oncology, 2019, 9, 7-13.	1.2	7
173	Technical Note: Dosimetric characterization of the dynamic beam flattening MLC sequence on a ring shaped, Jawless Linear Accelerator with double stacked MLC. Medical Physics, 2020, 47, 948-957.	1.6	7
174	Evaluation of Two-Voltage and Three-Voltage Linear Methods for Deriving Ion Recombination Correction Factors in Proton FLASH Irradiation. IEEE Transactions on Radiation and Plasma Medical Sciences, 2022, 6, 263-270.	2.7	7
175	A Volumetric Trend Analysis of the Prostate and Seminal Vesicles During a Course of Intensity-Modulated Radiation Therapy. American Journal of Clinical Oncology: Cancer Clinical Trials, 2010, 33, 173-175.	0.6	7
176	Oncology Scan—Improvements in Dose Calculation, Deformable Registration, and MR-Guided Radiation Delivery. International Journal of Radiation Oncology Biology Physics, 2013, 86, 395-397.	0.4	6
177	Higher Dose Volumes May Be Better for Evaluating Radiation Pneumonitis in Lung Proton Therapy Patients Compared With Traditional Photon-Based Dose Constraints. Advances in Radiation Oncology, 2020, 5, 943-950.	0.6	6
178	Dual-Energy Computed Tomography Proton-Dose Calculation with Scripting and Modified Hounsfield Units. International Journal of Particle Therapy, 2021, 8, 62-72.	0.9	6
179	Effects of motilin and ursodeoxycholic acid on gastrointestinal myoelectric activity of different origins in fasted rats. World Journal of Gastroenterology, 2004, 10, 2509.	1.4	6
180	A technique for reducing patient setup uncertainties by aligning and verifying daily positioning of a moving tumor using implanted fiducials. Journal of Applied Clinical Medical Physics, 2008, 9, 110-122.	0.8	5

#	Article	IF	CITATIONS
181	Predicting oropharyngeal tumor volume throughout the course of radiation therapy from pretreatment computed tomography data using general linear models. Medical Physics, 2014, 41, 051705.	1.6	5
182	Fetal dose from proton pencil beam scanning craniospinal irradiation during pregnancy: a Monte Carlo study. Physics in Medicine and Biology, 2022, 67, 035003.	1.6	5
183	Automating RTOG-defined target volumes for postmastectomy radiation therapy. Practical Radiation Oncology, 2011, 1, 97-104.	1.1	4
184	Improved human observer performance in digital reconstructed radiograph verification in head and neck cancer radiotherapy. International Journal of Computer Assisted Radiology and Surgery, 2015, 10, 1667-1673.	1.7	4
185	Initial Clinical Experience Treating Patients With Gynecologic Cancers on a 6MV Flattening Filter Free O-Ring Linear Accelerator. Advances in Radiation Oncology, 2020, 5, 920-928.	0.6	4
186	Daily Bone Alignment With Limited Repeat CT Correction Rivals Daily Ultrasound Alignment for Prostate Radiotherapy. International Journal of Radiation Oncology Biology Physics, 2008, 71, 274-280.	0.4	3
187	Fractionâ€variant beam orientation optimization for intensityâ€modulated proton therapy. Medical Physics, 2020, 47, 3826-3834.	1.6	3
188	Long-term Inter-protocol kV CBCT image quality assessment for a ring-gantry linac via automated QA approach. Biomedical Physics and Engineering Express, 2020, 6, 015025.	0.6	3
189	Tissue-specific deformable image registration using a spatial-contextual filter. Computerized Medical Imaging and Graphics, 2021, 88, 101849.	3.5	3
190	Emerging Technologies in Mitigating the Risks of Cardiac Toxicity From Breast Radiotherapy. Seminars in Radiation Oncology, 2022, 32, 270-281.	1.0	3
191	Forecasting longitudinal changes in oropharyngeal tumor morphology throughout the course of head and neck radiation therapy. Medical Physics, 2014, 41, 081708.	1.6	2
192	Initial clinical experience treating patients with palliative radiotherapy for malignant pleural mesothelioma on the HalcyonTM linear accelerator. Annals of Palliative Medicine, 2020, 9, 2903-2912.	0.5	2
193	Per-fraction positional and dosimetric performance of prone breast tangential radiotherapy on Halcyonâ,,¢ linear accelerator assessed with daily rapid kilo-voltage cone beam computed tomography: a single-institution pilot study. Radiation Oncology, 2020, 15, 258.	1.2	2
194	Cherenkov imaging for total skin electron therapy: an evaluation of dose uniformity. , 2021, 11628, .		2
195	Simultaneous Multiple Liver Metastasis Treated with Pencil Beam Proton Stereotactic Body Radiotherapy (SBRT). International Journal of Particle Therapy, 2021, 8, 89-94.	0.9	2
196	The distribution of motilin receptor in the amygdala of rats and its role in migrating myoelectric complex. Journal of Medical Colleges of PLA, 2007, 22, 329-336.	0.1	1
197	Anatomic variation and dosimetric consequences of neoadjuvant hormone therapy before radiation therapy for prostate cancer. Practical Radiation Oncology, 2013, 3, 329-336.	1.1	1
198	Efficient double-scattering proton therapy with a patient-specific bolus. Physica Medica, 2018, 50, 1-6.	0.4	1

#	Article	IF	CITATIONS
199	Initial Clinical Experience Treating Patients With Lung Cancer on a 6MV-Flattening-Filter-Free O-Ring Linear Accelerator. Cureus, 2020, 12, e10325.	0.2	1
200	Technical Note: Solving the "Chinese postman problem―for effective contour deformation. Medical Physics, 2018, 45, 767-772.	1.6	0
201	Abstract IA-019: Preclinical studies with proton FLASH radiotherapy in mice and canines: Biological effects, biophysical considerations and potential mechanisms. , 2021, , .		Ο
202	A Probability-Based Investigation on the Setup Robustness of Pencil-beam Proton Radiation Therapy for Skull-Base Meningioma. International Journal of Particle Therapy, 2021, 7, 34-45.	0.9	0
203	Advanced Topics in Particle Radiotherapy. IEEE Transactions on Radiation and Plasma Medical Sciences, 2022, 6, 247-251.	2.7	0